



# Facile fabrication of superhydrophobic paper with durability, chemical stability and self-cleaning by roll coating with modified nano-TiO<sub>2</sub>

Yuhong Teng<sup>1</sup> · Yufeng Wang<sup>1,2</sup> · Baoying Shi<sup>3</sup> · Weiwei Fan<sup>1</sup> · Ziyang Li<sup>1</sup> · Yunzhi Chen<sup>1</sup>

Received: 8 May 2020 / Accepted: 17 July 2020 / Published online: 29 July 2020  
© King Abdulaziz City for Science and Technology 2020

## Abstract

A superhydrophobic paper with excellent robustness was fabricated by roll coating with modified nano-TiO<sub>2</sub>. First, nano-TiO<sub>2</sub> particles were hydrophobically modified by  $\gamma$ -aminopropyltriethoxysilane and 1H, 1H, 2H, 2H-perfluorooctyltriethoxysilane (POTS). Then the paper coating composed of modified nano-TiO<sub>2</sub> particles as pigments and epoxy resin (EP) as adhesives was coated on a paper surface to create the desired surface morphology and surface energy. Compared with the uncoated filter paper, the prepared paper showed an improved rough surface morphology owing to the uniform layer of TiO<sub>2</sub> microclusters deposited on the fiber network. The superhydrophobic paper exhibited water contact angles (WCA) about  $153^\circ \pm 1.5^\circ$ , and water sliding angles (WSA) about  $3.5^\circ \pm 0.5^\circ$ , low surface adhesion and excellent bounce ability. The superhydrophobic paper can withstand a variety of wear and tear, such as tape stripping and knife scraping. The as-prepared superhydrophobic paper showed mechanical durability even after 20 wear cycles with sandpaper, thus sustaining excellent superhydrophobicity on the filter paper surface. Moreover, it remains fully functional even in environments with high concentrations of acid and alkali for 96 h. The superhydrophobicity was not affected after storage for 6 months in a natural environment. It was confirmed that the superhydrophobic paper surface exhibited excellent chemical stability, long-term stability and self-cleaning properties. The entire production process was operated under normal environment, without complex equipment; and, as such, has the possibility for large-scale production and application in industry.

**Keywords** TiO<sub>2</sub> nanoparticles · Superhydrophobicity · Paper substrate · Durability · Coating

## Introduction

The wetting property is a significant characteristic of solid surfaces and has an important impact on solving problems related to the health, environment, energy, transportation and biomedicine (Wen et al. 2017). When the water droplets are

on the solid surface, a contact angle can be measured at the edge of the water droplets, which is used to characterize the wettability of the water droplets (Celia et al. 2013). When the water contact angle (WCA) of the surface is more than  $150^\circ$  and the water sliding angle (WSA) is less than  $10^\circ$ , it is called superhydrophobic surface. Superhydrophobicity, as an extreme state of surface wettability, has attracted wide attention in the fields of anti-icing (Yang et al. 2020), drag reduction (Luo et al. 2020), anti-corrosion (Ren et al. 2020), selective absorption (Zhang et al. 2019a), self-cleaning (Xu et al. 2019) and so forth.

According to the theoretical equation of solid surface wettability and Wenzel and Cassie-Baxter models, a rough structure and low surface energy are prerequisites to produce superhydrophobic surfaces (Li et al. 2007). The high contact angle and micro-roughness ensure a small interface area, which reduces low adhesion. Up to now, researchers have employed a variety of physical or chemical methods including dip coating (Nguyen-Trig et al. 2019), template synthesis (Xu et al. 2020), laser ablation (Yang et al. 2019),

**Electronic supplementary material** The online version of this article (<https://doi.org/10.1007/s13204-020-01518-4>) contains supplementary material, which is available to authorized users.

✉ Yufeng Wang  
ppcwyf@tust.edu.cn

✉ Yunzhi Chen  
yzchen@tust.edu.cn

<sup>1</sup> Tianjin University of Science and Technology, Tianjin 300222, China

<sup>2</sup> State Key Lab of Pulp and Paper Engineering, South China University of Technology, Guangzhou 510640, China

<sup>3</sup> Tianjin Tianshi College, Tianjin 301700, China

sol–gel methods (Jiang et al. 2019), electrochemical deposition (Akbari et al. 2020), etc., to construct superhydrophobic surfaces on rigid substrates like metal, glass, silicon and so on.

Because of its biodegradability, renewability, wide availability, low-cost and easy modification of cellulose fibers, the paper has been considered an attractive material and can be used for more technical and professional uses (Li et al. 2017; Sousa and Mano 2013). However, the hygroscopicity and high moisture content of cellulose fibers resulting in poor physical properties of paper materials (Wang et al. 2019b). Since cellulose is the primary raw material for forming paper, it is easily destroyed by various methods including chemical, physical, and biological impact (Li et al. 2017), so many of the above manufacturing methods (Akbari et al. 2020; Jiang et al. 2019; Xu et al. 2020; Yang et al. 2019) cannot be used for fabrication of superhydrophobic paper. In recent years, some researchers have used layer-by-layer self-assembly technology (Li et al. 2017), the rapid expansion of supercritical solution (RESS) (Olin et al. 2015), non-solvent vapor method (Bai et al. 2018), etc. to construct superhydrophobic surfaces on paper substrates, but in many cases, the limitations of surface compatibility, complex preparation processes, high cost, and mass production limit the surface's real-world application. To promote the use of superhydrophobic paper in more fields, it is urgent to develop simple manufacturing methods (Zhang et al. 2017).

Fortunately, the paper is inherently rough and porous on a scale of a millimeter and micrometer, especially uncoated paper-like filter paper (Li et al. 2019d; Ou et al. 2019). According to the reported studies, some inorganic pigments such as  $\text{TiO}_2$ ,  $\text{ZnO}$ , and  $\text{Fe}_2\text{O}_3$  have been introduced to paper to create a dual sized roughness (Zhou et al. 2019). We used  $\text{TiO}_2$  as the superhydrophobic coating material owing to its large surface area, high surface activity (Foorginezhad and Zerafat 2019b), favorable physicochemical properties, non-toxicity and excellent stability (Gong et al. 2020). If nano titanium dioxide is modified by low surface energy substance such as perfluorosilane (Li et al. 2019d), then coated on filter paper by roll coating, a superhydrophobic surface on paper will be obtained theoretically. In terms of surface energy, the order  $-\text{CH}_2- > -\text{CH}_3 > -\text{CF}_2- > -\text{CF}_2\text{H} > -\text{CF}_3$  guides superhydrophobic scientific research, especially with fluorine-containing materials (Wang et al. 2015). Based on this surface energy order, we used 1H, 1H, 2H, 2H-perfluorooctyltriethoxysilane (POTS) as the superhydrophobic coating material. Compared with the research done by Lu et al. (2015) and Li et al. (2018), we first modified the nano- $\text{TiO}_2$  with  $\gamma$ -aminopropyltriethoxysilane and then modified them with low surface energy POTS. It not only improves the dispersion performance of nanoparticles in organic solvents but also achieves good hydrophobicity and expands the application of nanoparticles. In fact, roll coating using coatings

composed of pigments and adhesives is the most commonly used method to treat the paper surface in the paper industry, with most coated paper produced by roll coating. Especially, in roll coating process, the concentrations of inorganic pigments are more than 15 wt%, significantly higher than other coating methods such dip coating (Nguyen-Trig et al. 2019) and spray coating (Zhou et al. 2019), which ensured significant reduction of the amount of organic solvent. And up to now, there are few reports about the preparation of super-hydrophobic paper by the roll coating method. The mechanical robustness of superhydrophobic surfaces is also an extremely important issue for the widespread use of superhydrophobic materials in practical applications because most manufactured surface topography is easily damaged by mechanical wear during the use of the materials (Bai et al. 2018; Verho et al. 2011). Ogihara et al. (2012) used nanoparticles and silane to make superhydrophobic paper with early dissemination of mechanical robustness studies. Torun and Onses (2017) systematically investigated the robustness of the coatings using different tests. According to our preliminary study, traditional adhesives of a paper coating such as polyvinyl alcohol (PVA), starch and styrene-acrylic latex, do not achieve the desired effects. We find that a promising approach is using epoxy resin as an adhesive to optimize bond performance between the functionalized nanoparticles and paper surface.

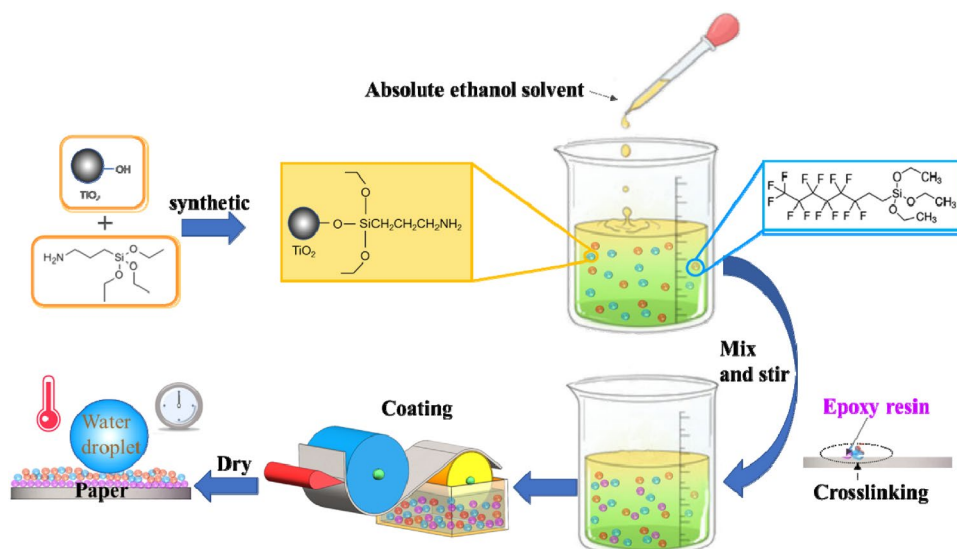
In this study, we demonstrated a facile and practical method to obtain superhydrophobic paper based on roll coating with nano- $\text{TiO}_2$  hydrophobically modified with  $\gamma$ -aminopropyltriethoxysilane and POTS, as illustrated in Scheme 1. Epoxy resin (EP) was used as a robust adhesive to optimize bond performance between nano titanium dioxide and paper. The superhydrophobic paper with multilayered micro/nano structure exhibited excellent hydrophobic stability, good wear resistance, chemical stability, stability and self-cleaning performance. It is expected that this novel process will provide an efficient method for fabricating durable superhydrophobic paper.

## Experimental section

### Materials

Absolute ethanol was obtained from Tianjin Fengchuan Chemical Reagent Science and Technology Co., Ltd.  $\gamma$ -aminopropyltriethoxysilane was obtained from Shanghai Yuanye Bio-Technology Co., Ltd.  $\text{TiO}_2$  nanoparticles (10–30 nm) was obtained from Beijing Deke Daojin Science and Technology Co., Ltd. Filter paper (medium speed) was obtained from Hangzhou Special Paper Co., Ltd.; POTS was purchased from Shanghai D&B Biological Science and Technology Co., Ltd.; epoxy resin was obtained from

**Scheme 1** Diagram for the process to produce superhydrophobic paper



Tianjin Heowns Biochem Technologies Co., Ltd.; sodium polyacrylate was obtained from Tianjin Solomon Biotechnology Co., Ltd.; and deionized water was obtained from Tianjin Kaisibo Biological Technology Co., Ltd.

### Preparation of superhydrophobic paper

0.3 g of  $\gamma$ -aminopropyltriethoxysilane and 100 mL of deionized water were mixed in a reaction vessel. After the prehydrolysis at 25 °C for 30 min with an ultrasonic dispersion analyzer at 100 Hz, Then 100 mL of absolute ethanol and 20 g of titanium dioxide were mixed with the hydrolysate. The system was then continuously stirred at 80 °C for 2 h to allow the additives to fully react. The reaction product was thoroughly centrifuged with ethanol and deionized water using a centrifuge to separate  $\gamma$ -aminopropyltriethoxysilane and other substances remaining in the reaction and dried in an oven at 80 °C for 5 h. The  $\gamma$ -aminopropyltriethoxysilane modified nanoparticles of TiO<sub>2</sub> were obtained as a white powder.

Then 1 g of POTS and 99 g of absolute ethanol were added to the reaction vessel and stirred for 2 h with a mechanical agitator. 20 g of  $\gamma$ -aminopropyltriethoxysilane modified TiO<sub>2</sub> nanoparticles were mixed to the solution obtained above. The reaction was conducted at 25 °C for 2 h with constant stirring. Then 2 g of epoxy resin as adhesive and 5 g sodium polyacrylate as dispersant were added. Everything in the system was then sonicated for 1 h and stirred for 4 h to produce a stable paper coating. The paper coating was applied on the surface of filter paper using a laboratory coater with a coating speed of 2 m/min and a coating amount of 12 g/m<sup>2</sup> by roll coating. The coated paper was then dried and solidified to obtain a superhydrophobic paper with a coating thickness of 13  $\mu$ m.

### Characterization

Surface morphologies of the superhydrophobic paper were observed by SEM (FEI\_Apereo, USA) at a voltage of 2 kV and magnification power of 1000 $\times$  and 200,000 $\times$ . The composition of the superhydrophobic paper was observed by EDS (FEI\_Apereo, USA). The roughness of the superhydrophobic paper was characterized by AFM (multimode8, American Brook). The crystal structure of TiO<sub>2</sub> nanoparticles was analyzed by XRD (D8 Advance, Bruker-AXS) with a scanning speed of 4°/min in the scanning range of 10°–80° (2 $\theta$ ). Functional groups and elemental analyses were performed by FTIR (Nicolet is5, America ThermoFisher) and XPS (Axis Ultra DLD Kratos AXIS SUPRA, UK). The WCAs of superhydrophobic paper surface were measured by VCA Optima dynamic contact angle tester (Optima, American AST) with 5  $\mu$ L water drops. The WSAs of superhydrophobic paper surface were measured by homemade test equipment with 60  $\mu$ L water drops. The valid values obtained were based on an average of at least five measurements. TG (TGA-Q50, USA) measurements were performed with a thermal analysis system under the protection of N<sub>2</sub> at a heating rate of 10 °C min<sup>-1</sup> from 30 to 600 °C. During the measurement, dried nitrogen was vented into the furnace at a constant flow rate of 50 mL min<sup>-1</sup>. The particle size of the nano-TiO<sub>2</sub> was tested by laser particle size analyzer (LS13 320, American Beckman Coulter).

## Results and discussion

### Physical parameters of coating

Paper coating is a mixed system composed of inorganic pigments and high molecular polymers. The physical

parameters of the coating can affect the quality of the coated products and the coating process (Torun et al. 2018). As shown in Table 1, the solids content of the coating is 27.2% and the viscosity of the coating is 2.89 Pa s, which meet the general requirements for paper coatings. After the TiO<sub>2</sub> nanoparticles are hydrophobically modified, the particle size measured by laser particle size analyzer is between 25.8 nm. Because the nanoparticles are difficult to disperse, the particle size covers a wide range. At the same time, after the coating was stored for 1 month, there was no clear change in appearance, no delamination, large particle aggregation, etc., which further supported the fact that the titanium dioxide nanoparticles were relatively stable in the coating system after hydrophobic modification, and could meet the requirements of industrial applications.

### Morphology and composition

The FT-IR spectra of TiO<sub>2</sub> before and after modification are shown in Fig. 1a. Compared with the original TiO<sub>2</sub>, the FT-IR spectrum of modified TiO<sub>2</sub> showed new weak peaks at 1047 cm<sup>-1</sup>, which belongs to the Si–O–Si band of KH550 (Mallakpour and Shahangi 2012). The peaks at 1243, 1211, and 1104 cm<sup>-1</sup> are the stretching vibration peaks of the C–F bonds, which exists as either a C–F<sub>2</sub> bond or a C–F<sub>3</sub> bond. This is due to the fluorination of the TiO<sub>2</sub> nanoparticles by POTS (Li and Guo 2019; Liu et al. 2019). The new peak at 1145 cm<sup>-1</sup> is the Si–O–C bond generated by the connection between POTS and TiO<sub>2</sub> nanoparticles (Brassard et al. 2011). These results indicate that the POTS has been attached to the surface of the TiO<sub>2</sub> by a covalent bond.

The XRD images of titanium dioxide before and after modification are displayed in Fig. 1b. It is worth noting that the original TiO<sub>2</sub> and modified TiO<sub>2</sub> spectra are similar and consistent with the standard PDF (JCPDS99-0008). According to the patterns, the major identical diffraction peaks appear in two curves at 25.3°, 37.8°, 48.0°, 53.9°, 55.1°, and 62.7°, corresponding to TiO<sub>2</sub> (101) (004), (200), (105), (211), (204), respectively. Apart from the main characteristic diffraction peaks of nano-TiO<sub>2</sub>, there are no other peaks, which shows that the sample is pure (Chen et al. 2015; Li et al. 2019a). Moreover, the crystal form of TiO<sub>2</sub> nanoparticles was not destroyed during the modification process, which means that the crystallinity of TiO<sub>2</sub> nanoparticles is not affected by  $\gamma$ -aminopropyltriethoxysilane and POTS modification (Su et al. 2018). According to the XRD analysis software MDI Jade, the crystal form of nano-TiO<sub>2</sub> is tetragonal, and the lattice constant is  $a = 3.785 \text{ \AA}$  and  $c = 9.514 \text{ \AA}$ .

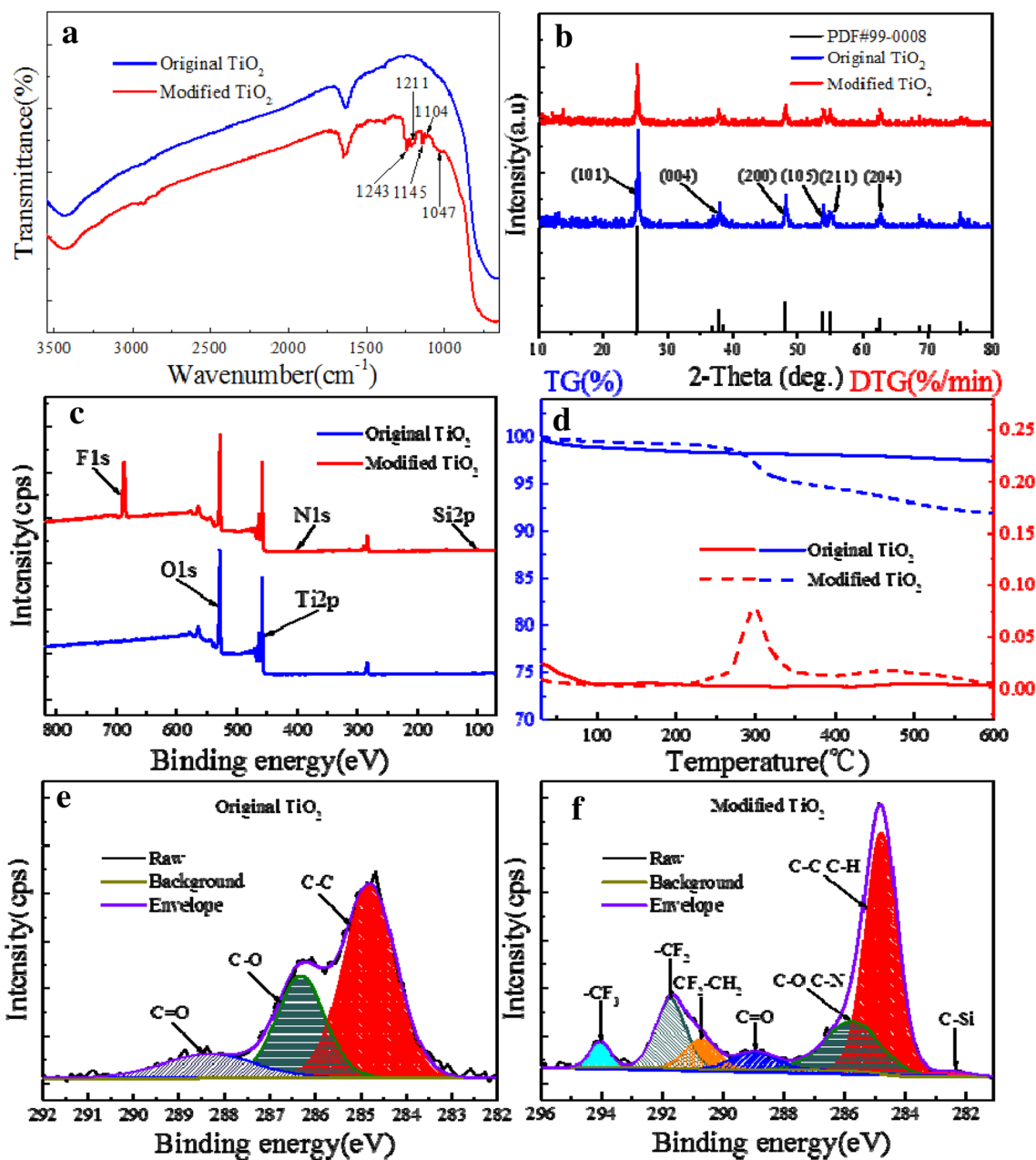
The XPS test was performed to characterize the chemical composition of TiO<sub>2</sub> before and after modification. The Si2p (102.07 eV) and N1s (400.04 eV) peaks (Fig. 1c) were observed for the modified TiO<sub>2</sub>. According to Table 2, their weight percentages (wt%) are 1.48, 0.95%, respectively. The C1s core-level spectrum of original and modified TiO<sub>2</sub> are shown in Fig. 1e, f. The high resolution C spectra of the original TiO<sub>2</sub> is fitted to three peaks at about 284.8, 286.33, and 288.734 eV (Guo et al. 2017; Lin et al. 2018), which were assigned to the C–C, C–O, and C=O, respectively (Fig. 1e). However, compared with Fig. 1f, two new component peaks appeared at 285.76 and 282.53 eV, corresponding to C–N and C–Si (Luo et al. 2020). The above results showed that the surface of nano titanium dioxide is covered with  $\gamma$ -aminopropyltriethoxysilane (Li et al. 2013). Moreover, F1s displayed one peak at binding energies of 688.78 eV (Fig. 1c). This peak has two different forms to coordinate with three components, which are 290.74 eV (CF<sub>2</sub>), 291.73 eV (CF<sub>2</sub>), and 294.05 eV (CF<sub>3</sub>), respectively (Miao et al. 2019). It turns out that the introduction of POTS results in the enrichment of F. It shows that POTS successfully modified TiO<sub>2</sub> particles and provided extremely low surface energy for the preparation of superhydrophobic surfaces (Li and Guo 2019).

Figure 1d showed the thermal stability of the original TiO<sub>2</sub> and modified TiO<sub>2</sub> as determined by TG analysis under N<sub>2</sub> protection conditions. TGA results show that the weight of the original TiO<sub>2</sub> did not change significantly over the whole temperature range from 30 to 600 °C. The weight loss of TiO<sub>2</sub> during the entire process is about 2.5% and is attributed to the reduction of hydroxyl groups on the titanium dioxide particle surface (Li et al. 2018). In the temperature range of 250–350 °C, the modified TiO<sub>2</sub> loses weight quickly. When the modified TiO<sub>2</sub> sample is heated to 600 °C, its weight loss is about 8%. The weight reduction of the modified TiO<sub>2</sub> is attributed to organic material on the sample surface, which decomposes between 250 and 600 °C (Wen and Guo 2018). Based on the above results, it can be explained that the addition of POTS increases the hydrophobicity of the modified TiO<sub>2</sub> but has a certain effect on thermal stability (Kang et al. 2019).

The surface morphology of filter paper before and after coating was characterized by SEM. The original filter paper consists of cellulose fibers, which are combined to form a fiber network and show a loose sheet structure (Fig. 2a) (Wang et al. 2019c). After coating with modified nano-TiO<sub>2</sub>, the entangled fibers are almost entirely covered by TiO<sub>2</sub> microclusters, which improves the

**Table 1** Physical parameters of coating

Test items	Solids content	Viscosity	Particle size	Stability
Experimental results	27.2%	2.89 Pa s	25.8 nm	No obvious change after a month



**Fig. 1** a FT-IR spectra of original TiO<sub>2</sub> and modified TiO<sub>2</sub>. b XRD of original TiO<sub>2</sub> and modified TiO<sub>2</sub>. c XPS images before and after TiO<sub>2</sub> modification. d TG/DTG curves of original TiO<sub>2</sub> and modified TiO<sub>2</sub>.

e C1s high-resolution XPS spectrum of the original TiO<sub>2</sub>. f C1s high-resolution XPS spectrum of the modified TiO<sub>2</sub>

**Table 2** Elemental composition of the original TiO<sub>2</sub> and modified TiO<sub>2</sub>

Sample	C1s (%)	O1s (%)	Ti2p (%)	Si2p (%)	N1s (%)	F1s (%)
Original TiO <sub>2</sub>	19.21	52.83	27.96	0	0	0
Modified TiO <sub>2</sub>	20.11	40.97	21.99	1.48	0.95	14.5

roughness and forms a dense rough structure (Fig. 2b) (Wang et al. 2019c). Figure 2d shows the morphology of the obtained paper surface more clearly, which

shows that the rough microstructure are mainly consists of nano-sized particles and micro-sized particles composed of nanoparticles and aggregated particles. It can



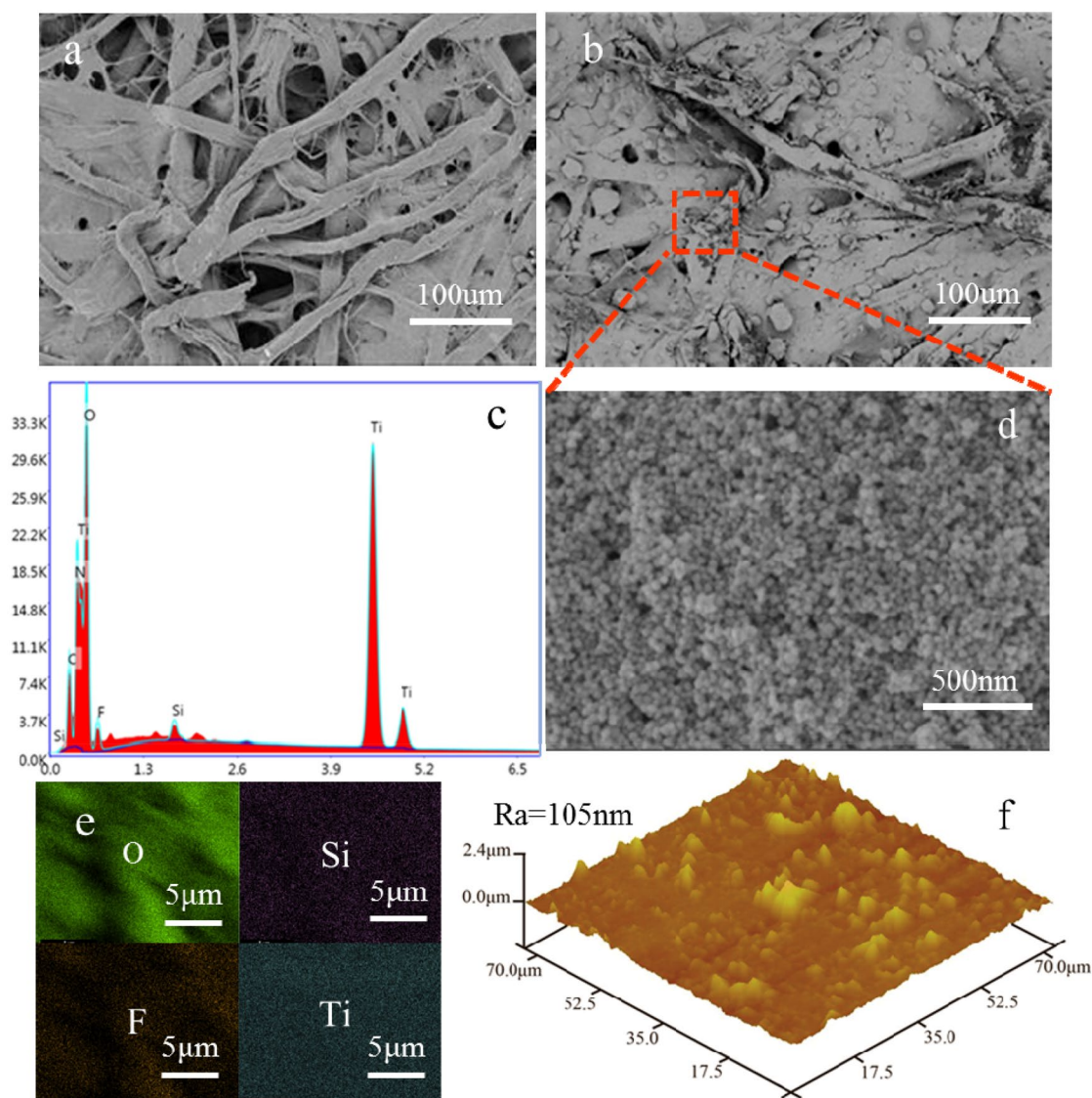


**Fig. 2** **a** SEM diagram of filter paper surface. **b** SEM image of superhydrophobic paper surface. **c** EDS spectra of superhydrophobic paper surface. **d** SEM images of superhydrophobic paper surface with

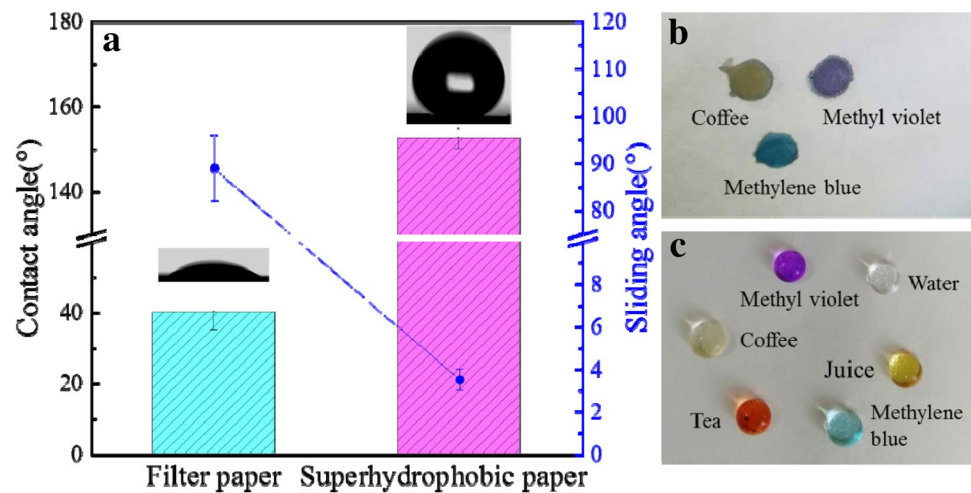
higher magnification. **e** EDS element distribution map of superhydrophobic paper surface. **f** AFM images of superhydrophobic paper surface

be seen from the EDS spectrum in Fig. 2c that the coating is composed of characteristic elements C, N, O, Ti, Si, and F. In addition, it is clear from Fig. 2d that Si, Ti, and F elements are uniformly distributed throughout the coating (Li et al. 2019b). Based on the data from AFM micrographs (Fig. 2f), the average roughness of the surface of the superhydrophobic paper was 105 nm, which is basically consistent with the particle size test (Table 1). This indicates that the modified TiO<sub>2</sub> produced lots of microclusters and formed micro-nano dual structure, indicating that the hydrophobicity is achieved through a dual structure (Zhi et al. 2017).

## Wettability

The wettability of filter paper and superhydrophobic paper surface were illustrated by tests of WCA and WSA (Fig. 3a). The WCA is approximately 39°, and the sliding angle is 89° on the filter paper surface. This is because cellulose is a structural polysaccharide which is composed of many hydroxyl groups (Wang et al. 2019c). The superhydrophobic paper surface has a WCA of  $153^\circ \pm 1.5^\circ$  and a WSA of  $3.5^\circ \pm 0.5^\circ$ . Figure 3b, c show the wettability behavior on different paper surfaces. The WSA on the superhydrophobic paper surface is small, showing very little adhesion of

**Fig. 3** **a** Variation diagram of WCA and WSA of filter paper and superhydrophobic paper. **b** Wettability behavior of filter paper surface. **c** Wettability behavior of superhydrophobic paper surface



water droplets (Yiqiang et al. 2016). On the prepared paper surface, beads prefer to jump on the surface rather than penetrating the surface. The Video Clip S1 mainly highlights the scene of water droplets rebounding on the surface of superhydrophobic paper. It can be observed that when a water drop falls from the lower part of the surface, it will immediately bounce off the surface. This proves the outstanding surface superhydrophobicity and the low adhesion ability of water droplets on the surface (Yiqiang et al. 2016). The explanation for the above result is that  $\text{TiO}_2$  micro-clusters are deposited on the fiber network, and a large number of protrusions and grooves are generated under the condition of air entrapment, thereby forming a micro/nanoscale roughness (Wang et al. 2019c; Zhang et al. 2018). This structure traps a lot of air into the coating and stops water from seeping into the trench, which causes water droplets to suspend on rough surfaces so that the prepared paper surface can form a higher WCA and a lower WSA (Wang et al. 2019c).

## Durability

Generally, there are many methods for characterizing the durability of superhydrophobic surface such as mechanical, chemical and long-term stability (Yang et al. 2017). The durability of prepared paper was demonstrated by abrasion test, immersion test and storage test. Superhydrophobic paper was tested by tape peeling and knife scratching. It can be seen from the Video Clip S2 that the superhydrophobic paper is fixed on a glass slide, peeled off with tape 20 times under a pressure of 1.2 kPa and scraped 10 times with a knife. After these durability tests, the superhydrophobic paper still maintained good water repellency and water droplets can slip off from the surface with a small angle. Figure 4c shows the abrasion test of superhydrophobic paper surface on sandpaper. The superhydrophobic paper with an area of  $2.5 \text{ cm} \times 2.5 \text{ cm}$  and a

weight of 100 g on the back was placed on sandpaper and moved 10 cm back and forth as a cycle (Fig. 4c). Figure 4a shows that the contact angle and rolling angle of coated paper without added adhesive have changed significantly while the angle of coated paper with added adhesive is still greater than  $150^\circ$  following 20 abrasion cycles, i.e. an abrasion distance of 400 cm. In Torun's study (Torun and Onses 2017), uncoated paper instead of sandpaper was used as an abrasive. A weight of 100 g was placed on the coated standard office paper with a wear distance of 100 cm and a wear area of  $10 \text{ cm} \times 2 \text{ cm}$ . The sliding angle of the water droplets ( $4 \mu\text{L}$ ) of the coated paper before wear is close to  $0^\circ$  and it was even difficult to measure the static water contact angle since the droplets immediately bounced off the substrate. After wear, the contact angle is  $151^\circ$  and the sliding angle is  $29^\circ$ . This indicates the mechanical wear-resisting of the as-prepared superhydrophobic surface has been greatly improved, and epoxy resin as an adhesive in the coating plays a key role. Meanwhile, compared with the study of Lu et al. (2015), the change in contact angle during sandpaper wear is smaller, indicating that the prepared coating has better mechanical stability. But epoxy resins containing hydrophilic groups and molecules with high surface energy as binders added to hydrophobic materials will reduce the hydrophobicity of the coating (Wu et al. 2018). Therefore, the contact angle of the coating is lowered. Moreover, Fig. 4d shows that after immersing in 0.1 mol/L HCl and 0.1 mol/L NaOH solution for 96 h, the WCA on the surface of the superhydrophobic paper remained above  $150^\circ$ . When the superhydrophobic paper was left at room temperature for 6 months, its contact angle was almost constant and it still had good hydrophobicity (Fig. 4e). These results indicate that the superhydrophobic paper still maintains good durability after being damaged in various ways.

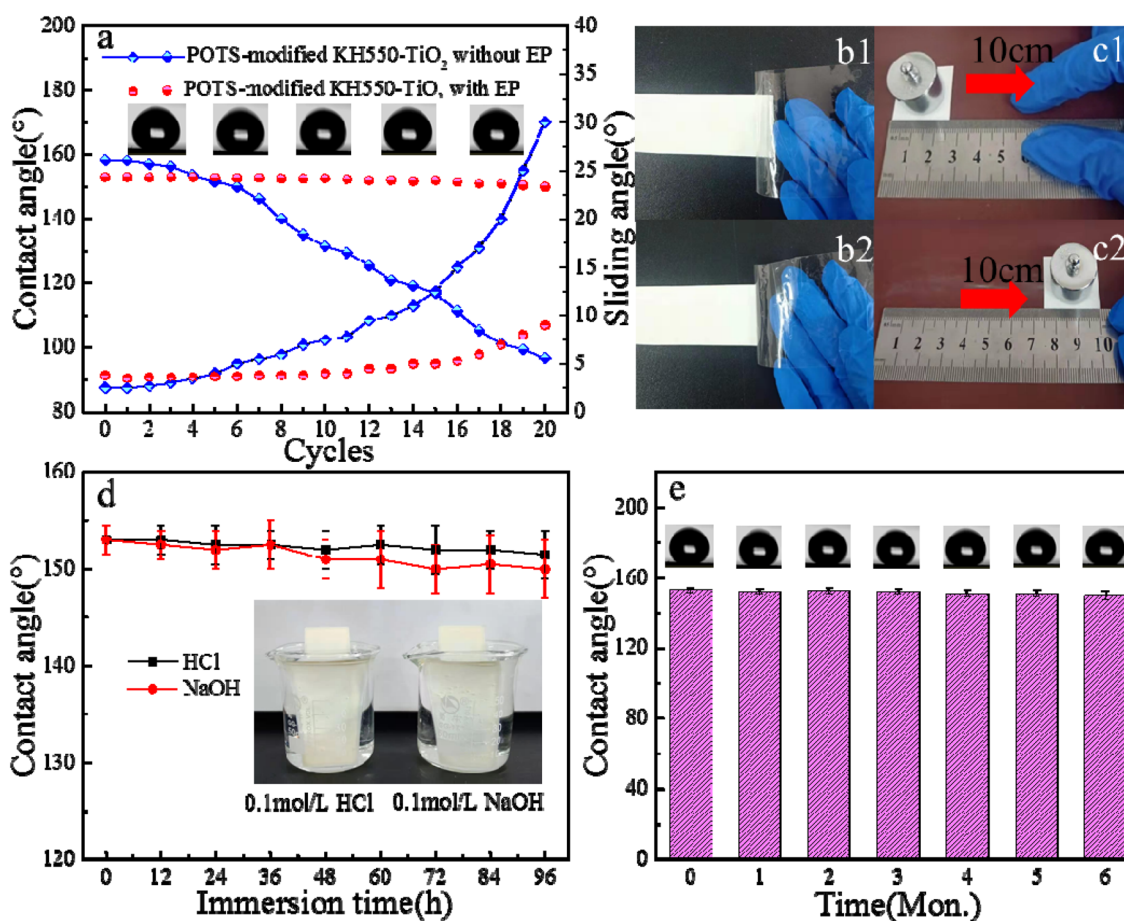


**Fig. 4** a Water contact angle under different abrasion cycles. b Tape peel test. c Abrasion test. d The change of WCA under different immersion time in 0.1 mol/L HCl and 0.1 mol/L NaOH (inset: the

optical photos of immersion). e Contact angle diagram for prepared paper stored for 1–6 months

## Self-cleaning

In practical applications, contamination on the solid surface is usually unavoidable (Latthe et al. 2019; Yang et al. 2019), so self-cleaning surfaces have an important impact in various fields. The soil and dust were used as research objects to assess the self-cleaning performance of superhydrophobic paper. Generally, a layer of soil and dust was scattered on superhydrophobic paper, and water droplets are allowed to fall on the surface of the contaminated superhydrophobic paper. Figure 5 illustrates the whole self-cleaning test, with the test sample as the one that was after 20 cycles of sand-paper wear test. We can see that when blue ink rolls off, the droplets take away the dirt and dust from the surface of the superhydrophobic paper, and the blue ink does not contaminate the sample surface. As shown in Video Clip S3, the contaminated superhydrophobic paper surface becomes gradually cleaner in the self-cleaning experiment. The above results can be explained by roughness and relatively low surface free energy of the superhydrophobic paper surfaces

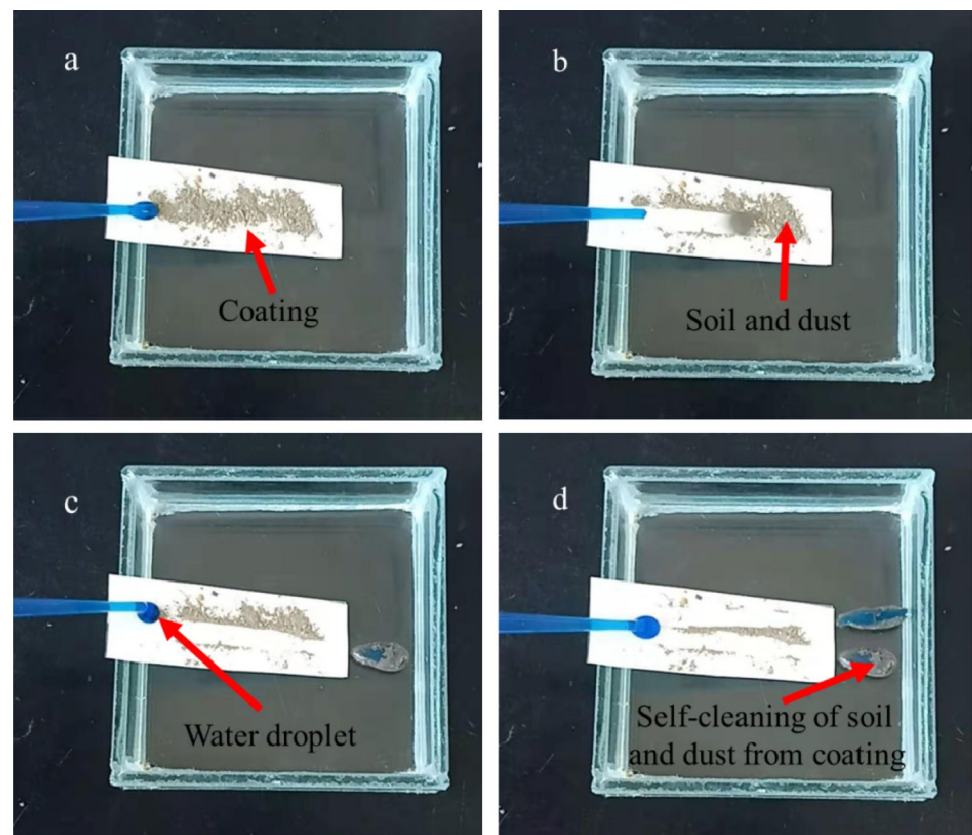
(Foorginezhad and Zerafat 2019a). It is well known that these properties will make the superhydrophobic paper surface have low adhesion (Wang et al. 2016).

## Current limitations and recommendation for possible future work

In recent years, various methods have been used to fabricate superhydrophobic paper surface, including coating (Khanjani et al. 2018; Torun and Onses 2017), layer-by-layer self-assembly technology (Li et al. 2017; Yang et al. 2017), chemical grafting modification (Li et al. 2012), rapid supercritical CO<sub>2</sub> expansion (Quan et al. 2009), colloid deposition (Geng et al. 2019), atom transfer radical polymerization (Verho et al. 2011), phase separation (Zhang et al. 2019b) and so on. However, most of the above methods require expensive instruments, the preparation process is complex, and mass production is limited. In this study, we demonstrated a facile and practical method to obtain superhydrophobic paper based on roll coating with nano-TiO<sub>2</sub> hydrophobically



**Fig. 5** Self-cleaning test chart for super-hydrophobic paper



modified with  $\gamma$ -aminopropyltriethoxysilane and POTS. Moreover, fluorides are widely used in the preparation of hydrophobic surfaces due to their low surface energy (Geng et al. 2019; Khanjani et al. 2018; Li et al. 2012; Peng et al. 2016; Torun and Onses 2017). However, fluorides have been banned to use by many countries because of their potential risk to organisms and the environment (Li et al. 2019c).

Although our work has addressed some of the above problems, some future work should focus on identifying a low-cost, fluorine-free and efficient multifunctional coating. PDMS is a good alternative to fluorine compounds since PDMS is inexpensive, hydrophobic, harmless, biocompatible, and widely used in industrial, daily life, and medical fields (Wang et al. 2019a). In addition, large-scale experiments should be carried out to demonstrate the technical feasibility and economics of the method we have developed.

## Conclusions

In summary, we developed a simple and practical method to fabricate robust superhydrophobic paper by roll coating with modified nano-TiO<sub>2</sub> particles as pigment and epoxy resin as adhesive. The WCA is 153° and the sliding angle is 3.5° on the fabricated superhydrophobic paper

surface. The superhydrophobic paper surface retained its superhydrophobicity after tape peeling, knife scratching, even after 20 sandpaper abrasion cycles. Furthermore, the superhydrophobic paper surface survived under immersion in acidic and alkaline solutions for 96 h, and after storing it for 6 months at room temperature, indicating its good chemical stability and long-term stability. In addition, the prepared superhydrophobic surface exhibited good self-cleaning performance. The prepared paper has the potential to be used in various applications because of its durability and self-cleaning performance. The entire production process was operated in an appropriate environment, without complex instrumentation; and has the possibility for large-scale production and application in industry.

**Acknowledgements** We would like to thank the supports from State Key Laboratory of Pulp and Paper Engineering (201615), Science project of Wuqing Science and Technology Commission of Tianjin (WQKJ201833), and Science Project of Tianjin Municipal Education Commission (2017KJ031).

## Compliance with ethical standards

**Conflict of interest** On behalf of all authors, the corresponding author states that there is no conflict of interest.

## References

- Akbari R, Godeau G, Mohammadzadeh M, Guittard F, Darmanin T (2020) The influence of bath temperature on the one-step electro-deposition of non-wetting copper oxide coatings. *Appl Surf Sci* 503:144094. <https://doi.org/10.1016/j.apsusc.2019.144094>
- Bai W, Guan M, Lai N, Yao R, Xu Y, Lin J (2018) Superhydrophobic paper from conjugated poly(*p*-phenylene)s: self-assembly and separation of oil/water mixture. *Mater Chem Phys* 216:230–236. <https://doi.org/10.1016/j.matchemphys.2018.06.014>
- Brassard JD, Sarkar DK, Perron J (2011) Synthesis of monodisperse fluorinated silica nanoparticles and their superhydrophobic thin films. *ACS Appl Mater Interfaces* 3:3583–3588. <https://doi.org/10.1021/am2007917>
- Celia E, Darmanin T, Taffin de Givenchy E, Amigoni S, Guittard F (2013) Recent advances in designing superhydrophobic surfaces. *J Colloid Interface Sci* 402:1–18. <https://doi.org/10.1016/j.jcis.2013.03.041>
- Chen Y, Li F, Cao W, Li T (2015) Preparation of recyclable CdS photocatalytic and superhydrophobic films with photostability by using a screen-printing technique. *J Mater Chem A* 3:16934–16940. <https://doi.org/10.1039/c5ta04065e>
- Foorginezhad S, Zerafat MM (2019a) Fabrication of stable fluorine-free superhydrophobic fabrics for anti-adhesion and self-cleaning properties. *Appl Surf Sci* 464:458–471. <https://doi.org/10.1016/j.apsusc.2018.09.058>
- Foorginezhad S, Zerafat MM (2019b) Fabrication of superhydrophobic coatings with self-cleaning properties on cotton fabric based on Octa vinyl polyhedral oligomeric silsesquioxane/polydimethylsiloxane (OV-POSS/PDMS) nanocomposite. *J Colloid Interface Sci* 540:78–87. <https://doi.org/10.1016/j.jcis.2019.01.007>
- Geng YY, Li JH, Li Z, Chen MM, Zhao HG, Zhang L (2019) Facile preparation of 3D graphene-based/polyvinylidene fluoride composite for organic solvents capture in spent fuel reprocessing. *J Porous Mater* 26:1619–1629. <https://doi.org/10.1007/s10934-019-00760-8>
- Gong Z, Yang N, Chen Z, Jiang B, Sun Y, Yang X, Zhang L (2020) Fabrication of meshes with inverse wettability based on the TiO<sub>2</sub> nanowires for continuous oil/water separation. *Chem Eng J* 380:122524. <https://doi.org/10.1016/j.cej.2019.122524>
- Guo XJ, Xue CH, Jia ST, Ma JZ (2017) Mechanically durable super-amphiphobic surfaces via synergistic hydrophobization and fluorination. *Chem Eng J* 320:330–341. <https://doi.org/10.1016/j.cej.2017.03.058>
- Jiang C, Liu W, Sun Y, Liu C, Yang M, Wang Z (2019) Fabrication of durable superhydrophobic and superoleophilic cotton fabric with fluorinated silica sol via sol–gel process. *J Appl Polym Sci* 136:47005. <https://doi.org/10.1002/app.47005>
- Kang L et al (2019) A water solvent-assisted condensation polymerization strategy of superhydrophobic lignocellulosic fibers for efficient oil/water separation. *J Mater Chem A* 7:16447–16457. <https://doi.org/10.1039/c9ta04815d>
- Khanjani P, King AWT, Partl GJ, Johansson LS, Kostianin MA, Ras RHA (2018) Superhydrophobic paper from nanostructured fluorinated cellulose esters. *ACS Appl Mater Interfaces* 10:11280–11288. <https://doi.org/10.1021/acsami.7b19310>
- Latthe SS et al (2019) Self-cleaning superhydrophobic coatings: potential industrial applications. *Prog Org Coat* 128:52–58. <https://doi.org/10.1016/j.porgcoat.2018.12.008>
- Li Q, Guo Z (2019) A highly fluorinated SiO<sub>2</sub> particle assembled, durable superhydrophobic and superoleophobic coating for both hard and soft materials. *Nanoscale* 11:18338–18346. <https://doi.org/10.1039/c9nr07435j>
- Li Y, Huang XJ, Heo SH, Li CC, Choi YK, Cai WP, Cho SO (2007) Superhydrophobic bionic surfaces with hierarchical microsphere/SWCNT composite arrays. *Langmuir* 23:2169–2174. <https://doi.org/10.1021/la0620758>
- Li J, Wan HQ, Ye YP, Zhou HD, Chen JM (2012) One-step process to fabrication of transparent superhydrophobic SiO<sub>2</sub> paper. *Appl Surf Sci* 261:470–472. <https://doi.org/10.1016/j.apsusc.2012.08.034>
- Li XW, Song RG, Jiang Y, Wang C, Jiang D (2013) Surface modification of TiO<sub>2</sub> nanoparticles and its effect on the properties of fluoropolymer/TiO<sub>2</sub> nanocomposite coatings. *Appl Surf Sci* 276:761–768. <https://doi.org/10.1016/j.apsusc.2013.03.167>
- Li H, Yang J, Li P, Lan T, Peng L (2017) A facile method for preparation superhydrophobic paper with enhanced physical strength and moisture-proofing property. *Carbohydr Polym* 160:9–17. <https://doi.org/10.1016/j.carbpol.2016.12.018>
- Li C, Sun Y, Cheng M, Sun S, Hu S (2018) Fabrication and characterization of a TiO<sub>2</sub>/polysiloxane resin composite coating with full-thickness super-hydrophobicity. *Chem Eng J* 333:361–369. <https://doi.org/10.1016/j.cej.2017.09.165>
- Li C et al (2019a) Facile preparation of TiO<sub>2</sub>/acrylic resin superhydrophobic surface with excellent wear resistance. *J Appl Polym Sci* 136:47762. <https://doi.org/10.1002/app.47762>
- Li D-W, Wang H-Y, Liu Y, Wei D-S, Zhao Z-X (2019b) Large-scale fabrication of durable and robust super-hydrophobic spray coatings with excellent repairable and anti-corrosion performance. *Chem Eng J* 367:169–179. <https://doi.org/10.1016/j.cej.2019.02.093>
- Li SN, Zhong L, Huang S, Wang DF, Zhang FX, Zhang GX (2019c) A reactive fluorine-free, efficient superhydrophobic and flame-retardant finishing agent for cotton fabrics. *Cellulose* 26:6333–6347. <https://doi.org/10.1007/s10570-019-02503-z>
- Li Z, Yang X, Li W, Liu H (2019d) Stimuli-responsive cellulose paper materials. *Carbohydr Polym* 210:350–363. <https://doi.org/10.1016/j.carbpol.2019.01.082>
- Lin DM, Zeng XR, Li HQ, Lai XJ (2018) Facile fabrication of superhydrophobic and flame-retardant coatings on cotton fabrics via layer-by-layer assembly. *Cellulose* 25:3135–3149. <https://doi.org/10.1007/s10570-018-1748-9>
- Liu H et al (2019) Silica coating with well-defined micro-nano hierarchy for universal and stable surface superhydrophobicity. *Chem Phys Lett* 730:594–599. <https://doi.org/10.1016/j.cplett.2019.06.001>
- Lu Y, Sathasivam S, Song J, Crick CR, Carmalt CJ, Parkin IP (2015) Robust self-cleaning surfaces that function when exposed to either air or oil. *Science* 347:1132–1135. <https://doi.org/10.1126/science.aaa0946>
- Luo G, Wen L, Yang K, Li X, Xu S, Pi P, Wen X (2020) Robust and durable fluorinated 8-MAPOSS-based superamphiphobic fabrics with buoyancy boost and drag reduction. *Chem Eng J* 383:123125. <https://doi.org/10.1016/j.cej.2019.123125>
- Mallakpour S, Shahangi V (2012) Modification of clay with L-leucine and TiO<sub>2</sub> with silane coupling agent for preparation of poly(vinyl alcohol)/organo-nanoclay/modified TiO<sub>2</sub> nanocomposites film. *Des Monomers Polym* 15:329–344. <https://doi.org/10.1163/156855511x615713>
- Miao Y et al (2019) Mussel-inspired superhydrophobic surfaces on 316L stainless steel with enhanced corrosion resistance. *Metall and Mater Trans A* 51:909–919. <https://doi.org/10.1007/s11661-019-05573-7>
- Nguyen-Trig P, Altiparmak F, Nguyen N, Tuduri L, Ouellet-Plamondon CM, Prud'homme RE (2019) Robust superhydrophobic cotton fibers prepared by simple dip-coating approach using chemical and plasma-etching pretreatments. *ACS Omega* 4:7829–7837. <https://doi.org/10.1021/acsomega.9b00688>
- Ogihara H, Xie J, Okagaki J, Saji T (2012) Simple method for preparing superhydrophobic paper: spray-deposited hydrophobic silica nanoparticle coatings exhibit high water-repellency and transparency. *Langmuir* 28:4605–4608. <https://doi.org/10.1021/la204492q>

- Olin P, Hyll C, Ovaskainen L, Ruda M, Schmidt O, Turner C, Wagberg L (2015) Development of a semicontinuous spray process for the production of superhydrophobic coatings from supercritical carbon dioxide solutions. *Ind Eng Chem Res* 54:1059–1067. <https://doi.org/10.1021/ie503798k>
- Ou J, Wu B, Wang F, Xue M (2019) Textile with Janus wetting properties via copper deposition and subsequent chemical vapor deposition of 1-dodecanethiol. *Mater Lett* 251:5–7. <https://doi.org/10.1016/j.matlet.2019.04.105>
- Peng L, Lei WK, Yu P, Luo YB (2016) Polyvinylidene fluoride (PVDF)/hydrophobic nano-silica (H-SiO<sub>2</sub>) coated superhydrophobic porous materials for water/oil separation. *RSC Adv* 6:10365–10371. <https://doi.org/10.1039/c5ra17728f>
- Quan C, Werner O, Wagberg L, Turner C (2009) Generation of superhydrophobic paper surfaces by a rapidly expanding supercritical carbon dioxide-alkyl ketene dimer solution. *J Supercrit Fluids* 49:117–124. <https://doi.org/10.1016/j.supflu.2008.11.015>
- Ren B, Chen Y, Li Y, Li W, Gao S, Li H, Cao R (2020) Rational design of metallic anti-corrosion coatings based on zinc gluconate@ZIF-8. *Chem Eng J* 384:123389. <https://doi.org/10.1016/j.cej.2019.123389>
- Sousa MP, Mano JF (2013) Superhydrophobic paper in the development of disposable labware and lab-on-paper devices. *ACS Appl Mater Interfaces* 5:3731–3737. <https://doi.org/10.1021/am400343n>
- Su XJ et al (2018) Dual-functional superhydrophobic textiles with asymmetric roll-down/pinned states for water droplet transportation and oil–water separation. *ACS Appl Mater Interfaces* 10:4213–4221. <https://doi.org/10.1021/acsami.7b15909>
- Torun I, Onses MS (2017) Robust superhydrophobicity on paper: protection of spray-coated nanoparticles against mechanical wear by the microstructure of paper. *Surf Coat Technol* 319:301–308. <https://doi.org/10.1016/j.surfcoat.2017.04.009>
- Torun I, Celik N, Hancer M, Es F, Emir C, Turan R, Onses MS (2018) Water impact resistant and antireflective superhydrophobic surfaces fabricated by spray coating of nanoparticles: interface engineering via end-grafted polymers. *Macromolecules* 51:10011–10020. <https://doi.org/10.1021/acs.macromol.8b01808>
- Verho T, Bower C, Andrew P, Franssila S, Ikkala O, Ras RHA (2011) Mechanically durable superhydrophobic surfaces. *Adv Mater* 23:673–678. <https://doi.org/10.1002/adma.201003129>
- Wang H, Chen E, Jia X, Liang L, Wang Q (2015) Superhydrophobic coatings fabricated with polytetrafluoroethylene and SiO<sub>2</sub> nanoparticles by spraying process on carbon steel surfaces. *Appl Surf Sci* 349:724–732. <https://doi.org/10.1016/j.apsusc.2015.05.068>
- Wang HY, Zhang XG, Liu ZJ, Zhu YX, Wu SQ, Zhu YJ (2016) A superrobust superhydrophobic PSU composite coating with self-cleaning properties, wear resistance and corrosion resistance. *RSC Adv* 6:10930–10937. <https://doi.org/10.1039/c5ra22396b>
- Wang B, Peng S, Wang Y, Li X, Zhang K, Liu C (2019a) A non-fluorine method for preparing multifunctional robust superhydrophobic coating with applications in photocatalysis, flame retardance, and oil–water separation. *New J Chem* 43:7471–7481. <https://doi.org/10.1039/c9nj01318k>
- Wang Q, Xiong J, Chen G, Xinping O, Yu Z, Chen Q, Yu M (2019b) Facile approach to develop hierarchical roughness fiber@SiO<sub>2</sub> blocks for superhydrophobic paper. *Materials* 12:1393. <https://doi.org/10.3390/ma12091393>
- Wang Y, Liu Y, Zhang L, Zhang M, He G, Sun Z (2019c) Facile fabrication of a low adhesion, stable and superhydrophobic filter paper modified with ZnO microclusters. *Appl Surf Sci* 496:143743. <https://doi.org/10.1016/j.apsusc.2019.143743>
- Wen G, Guo Z (2018) Nonflammable superhydrophobic paper with biomimetic layered structure exhibiting boiling–water resistance and repairable properties for emulsion separation. *J Mater Chem A* 6:7042–7052. <https://doi.org/10.1039/c8ta01920g>
- Wen G, Guo Z, Liu W (2017) Biomimetic polymeric superhydrophobic surfaces and nanostructures: from fabrications to applications. *Nanoscale* 9:3338–3366. <https://doi.org/10.1039/c7nr00096k>
- Wu YH et al (2018) Superhydrophobic modification of cellulose film through light curing polyfluoro resin in situ. *Cellulose* 25:1617–1623. <https://doi.org/10.1007/s10570-018-1676-8>
- Xu S, Wang Q, Wang N, Zheng X (2019) Fabrication of superhydrophobic green surfaces with good self-cleaning, chemical stability and anti-corrosion properties. *J Mater Sci* 54:13006–13016. <https://doi.org/10.1007/s10853-019-03789-x>
- Xu WT, Yi PY, Gao J, Deng YJ, Peng LF, Lai XM (2020) Large-area stable superhydrophobic poly(dimethylsiloxane) films fabricated by thermal curing via a chemically etched template. *ACS Appl Mater Interfaces* 12:3042–3050. <https://doi.org/10.1021/acsami.9b19677>
- Yang J, Li H, Lan T, Peng L, Cui R, Yang H (2017) Preparation, characterization, and properties of fluorine-free superhydrophobic paper based on layer-by-layer assembly. *Carbohydr Polym* 178:228–237. <https://doi.org/10.1016/j.carbpol.2017.09.040>
- Yang Z, Liu X, Tian Y (2019) Hybrid laser ablation and chemical modification for fast fabrication of bio-inspired super-hydrophobic surface with excellent self-cleaning, stability and corrosion resistance. *J Bionic Eng* 16:13–26. <https://doi.org/10.1007/s42235-019-0002-y>
- Yang C et al (2020) Functionalized CFRP surface with water-repellence, self-cleaning and anti-icing properties. *Colloids Surf A* 586:124278. <https://doi.org/10.1016/j.colsurfa.2019.124278>
- Yiqiang W, Shanshan J, Yan Q, Sha L, Ming L (2016) A versatile and efficient method to fabricate durable superhydrophobic surfaces on wood, lignocellulosic fiber, glass, and metal substrates. *J Mater Chem A* 4:14111–14121. <https://doi.org/10.1039/c6ta05259b>
- Zhang X, Batchelor W, Shen W (2017) Building dual-scale roughness using inorganic pigments for fabrication of superhydrophobic paper. *Ind Eng Chem Res* 56:3618–3628. <https://doi.org/10.1021/acs.iecr.7b00225>
- Zhang Y, Ren FL, Liu YJ (2018) A superhydrophobic EP/PDMS nanocomposite coating with high gamma radiation stability. *Appl Surf Sci* 436:405–410. <https://doi.org/10.1016/j.apsusc.2017.12.019>
- Zhang X, Liu Z, Li Y, Wang C, Zhu Y, Wang H, Wang J (2019a) Robust superhydrophobic epoxy composite coating prepared by dual interfacial enhancement. *Chem Eng J* 371:276–285. <https://doi.org/10.1016/j.cej.2019.04.040>
- Zhang YP et al (2019b) Fast and simple fabrication of superhydrophobic coating by polymer induced phase separation. *Nanomaterials* 9:411. <https://doi.org/10.3390/nano9030411>
- Zhi D, Lu Y, Sathasivam S, Parkin IP, Zhang X (2017) Large-scale fabrication of translucent and repairable superhydrophobic spray coatings with remarkable mechanical, chemical durability and UV resistance. *J Mater Chem A* 5:10622–10631. <https://doi.org/10.1039/c7ta02488f>
- Zhou X, Yu S, Zang J, Lv Z, Liu E, Zhao Y (2019) Colorful nanostructured TiO<sub>2</sub> film with superhydrophobic–superhydrophilic switchable wettability and anti-fouling property. *J Alloy Compd* 798:257–266. <https://doi.org/10.1016/j.jallcom.2019.05.259>

**Publisher's Note** Springer Nature remains neutral with regard to jurisdictional claims in published maps and institutional affiliations.